The factors related to carbon dioxide effluxes and production in the soil profiles of rain-fed maize fields

Weige Nan[a,c], Shanchao Yue[a,b], Shiqing Li[a,b,*], Haizhou Huang[b], Yufang Shen[a,b]

[a] State Key Laboratory of Soil Erosion and Dryland Farming on the Loess Plateau, Institute of Soil and Water Conservation, Chinese Academy of Sciences and Ministry of Water Resources, Yangling, Shaanxi 712100, China
[b] Institute of Soil and Water Conservation, Northwest A&F University, Yangling, Shaanxi 712100, China
[c] University of Chinese Academy of Sciences, Beijing, 100049, China

A B S T R A C T

We assessed soil carbon dioxide (CO_2) production and transport in high-yield fields and confirmed the main sources and main driving factors of CO_2 at different soil depths. Our experiments were performed at the Changwu ecological station, and we utilized a 3-year-old fertility experiment to study the production and effluxes of CO_2 within soil profiles. Soil CO_2 efflux rates were computed by the concentration gradient method, where CO_2 concentrations were measured using flame ionization detector (FID) from situ gas samplers. The results showed that the cumulative production and effluxes of CO_2 in the soil decreased with depth; most of CO_2 soil production and effluxes occurred in the surface soil (0–15 cm), where the cumulative production and effluxes of CO_2 accounted for 72.3% and 76.3% of the total amounts in the soil profile (0–100 cm), respectively. Higher efflux rates were observed with high production rates from the sixth-leaf stage (V6) to the silking stage (R1), which is a period of rapid maize growth and soil water stress. During that period, mean cumulative effluxes accounted for 52–57% of the annual effluxes. The application of nitrogen fertilizer strongly improved plant growth and grain yield and slightly promoted CO_2 production and effluxes. However, nitrogen fertilizer application did not affect the productive contribution rate, i.e., the contribution rate of CO_2 production in each soil layer to the entire profile (% of total), which revealed that the production and effluxes of CO_2 responded weakly to nitrogen fertilizer. The integrated application of manure and nitrogen fertilizer significantly increased the production and effluxes of CO_2 within the soil profiles and significantly improved the productive contribution rates of CO_2 in the topsoil. In addition, manure application promoted much greater soil CO_2 production throughout the observation period, so the contribution from manure was greater than that from nitrogen fertilizer.

© 2015 Elsevier B.V. All rights reserved.

1. Introduction

Soils are a major source of atmospheric carbon dioxide (CO_2), contributing 60–70 Pg CO_2–C yr^{-1} (Allen et al., 2009; Schlesinger and Andrews, 2000), and minor changes in the balance between belowground carbon storage and release can have major impacts on CO_2 emissions. Vast quantities of carbon in the form of roots and decomposed organic matter are stored in the soil, and carbon is released into the atmosphere as CO_2 through physical, chemical, and biological processes, which result in a balance between the storage of organic carbon compounds and their emission (Johnston et al., 2004). Soil CO_2 emission is often referred to as soil respiration, which is typically classified as autotrophic (from plant roots and the rhizosphere) or heterotrophic (from soil organisms ranging in size from bacteria to fungi, small insects, and small mammals) (Trumbore, 1993). Crops directly affect autotrophic respiration, and crop residues affect heterotrophic respiration (Hassan et al., 2014; Schulz et al., 2011; Vargas et al., 2014). However, environmental factors, such as soil temperature, moisture, and organic matter, can also affect soil respiration (Bond-Lamberty and Thomson, 2010; Cook et al., 1998; Davidson et al., 1998, 2000, 2006; Davidson and Janssens, 2006; Liu et al., 2012; Fang et al., 2009; Fang and Moncrieff, 2001; Gaumont-Guay et al., 2006; Jassal et al., 2004; Kirschbaum, 1995), and manures support rich microbial communities (Elhottová et al., 2012) and provide many different types of organic matter (Šimek et al., 2014),

* Corresponding author at: State Key Laboratory of Soil Erosion and Dryland Farming on the Loess Plateau, Institute of Soil and Water Conservation, Chinese Academy of Sciences and Ministry of Water Resources, Yangling, Shaanxi 712100, China. Fax: +86 29 87016171.
E-mail address: sqli@ms.iswc.ac.cn (S. Li).

which is an important source of CO_2 (Hynšt et al., 2007; Xu et al., 2011). Fertilizer inputs increase soil N availability, which can affect crop growth and the microbial community and accelerate the decomposition of soil organic matter, thereby affecting soil respiration (Ramirez et al., 2010; Xu et al., 2011). Thus, we conceived an experiment to identify and measure the major factors that affect CO_2 production, including plant growth, soil temperature and water content, from the application of organic fertilizer and N fertilizer.

Net soil surface gas fluxes result from the production and transportation of gases through the underlying soil (Bowden and Bormann, 1986), and soil CO_2 is produced at all depths and transported to the soil surface. To understand when and how soil CO_2 is produced at different depths, it is necessary to determine both the soil CO_2 concentration and the CO_2 efflux of the soil profile (Fierer et al., 2005; Jassal et al., 2005; Kusa et al., 2010; Novak, 2007; Risk et al., 2002a,b; Shrestha et al., 2004). Some studies have undertaken field observations to highlight the importance of the vertical distribution of CO_2 concentrations and their flux, which is generally derived from Fick's first law, on soil CO_2 efflux. Hendry et al. (1999) simulated soil CO_2 concentration and soil-surface CO_2 flux and quantified the CO_2 production rate at each depth using parameterization and sensitivity analysis. Some studies have also investigated the relative contribution of different soil depths to the total CO_2 production of a soil profile (Hashimoto et al., 2007). For example, Davidson and Trumbore (1995) found that approximately 70–80% of the CO_2 production in forests and pasture in the Amazon basin occurs within the top 100 cm of soil, and Gaudinski et al. (2000) found that 63% of soil respiration occurs in the top 15 cm of the soil in a temperate forest. Davidson et al. (2006) estimated that the O horizon (the organic horizon, which is 3–8 cm thick) contributes 40–48% of the total annual soil CO_2 efflux in a mixed hardwood stand in Massachusetts, and Fierer et al. (2005) revealed that the CO_2 production in the subsurface (soil below 40 cm in depth) at a California grassland site equals half of the CO_2 flux when surface conditions are water-limited. However, few studies have investigated CO_2 production and effluxes in the soil profiles in an agro-ecosystem. Supplemental fertilizer can enhance agricultural production, but its impact on CO_2 effluxes and production remains unclear. Thus, it is necessary to investigate the CO_2 production from soil profiles under different fertilization regimes.

The Loess Plateau covers an area of 623,800 km^2 in northwest China suffers from serious soil erosion and low productivity (Li and Xiao, 1992), so the land must be enhanced through fertilization and reduced CO_2 efflux (Chen et al., 2014; Rustad et al., 2000; Tilman et al., 2002). We had previously constructed a high-yield and high-efficiency hybrid maize production system and found that the grain yield in the area increased with increasing rates of N application. Higher N application (i.e., 380 kg N ha^{-1}, N380) practices could achieve high yields but might pose environmental risks, such as nitrogen surpluses, nitrate leaching, ammonia volatilization and N_2O emissions (Liu et al., 2014a). Nevertheless, grain yield peaked as a result of the integrated application of manure and N (250 kg N ha^{-1}, MN250), in which the N input was nearly equivalent to the N uptake by the maize, which resulted in lower N_2O emissions (Liu et al., 2014b). Using the two treatments in the high-N and high-efficiency plot, we investigated the influence of fertilizer application on the soil effluxes and production of CO_2 to further understand the main controlling factors by analyzing plant growth, soil temperature, soil water-filled pore space (WFPS) and water-soluble organic carbon (WSOC). Based on changes in the CO_2 concentrations in the profile soil with depth and over time, we calculated the CO_2 efflux by Fick's first law and determined CO_2 production to enhance our understanding of the net carbon flux at the interface of the soil and atmosphere. This information could enable the development of measures to abate CO_2 effluxes.

2. Experiments

2.1. Site description

The experiment was performed between 2012 and 2013 at the Changwu Agro-ecological Station on the Loess Plateau (35.28°N, 107.88°E and approximately 1200 m ASL). The station is located in a typical semiarid farming area with an average annual precipitation of 582 mm and an average annual temperature of 9.2 °C; the frost-free period is 171 days. One crop is planted per year (wheat or maize), and according to the Chinese soil taxonomy, the soils at the study site are Cumuli-Ustic Isohumosols (Gong et al., 2007). The annual precipitation was 480.8 mm in 2012 and 577.3 mm in 2013 with 75.6% and 71.3%, respectively, falling during the maize growing season. The daily average air temperature changed from approximately -5.0 °C in January to approximately 23 °C in August (air temperature data were missing from May 7th to June 6th in 2013, due to equipment failure). The experimental soil was identified before planting in 2009 and found to contain 4% sand, 59% silt and 37% clay. The soil in the top 20 cm had a bulk density of 1.3 g cm^{-3}, a pH of 8.4, an organic matter content of 16.4 g kg^{-1}, a total N content of 1.05 g kg^{-1}, an Olsen-P content of 20.7 mg kg^{-1}, an NH_4OAc-extractable K content of 133.1 mg kg^{-1}, and a mineral N content of 28.8 mg kg^{-1}.

2.2. Experimental design and crop management

The field experiment was situated within 50 m of the experimental site and composed of the following three treatments: no N applied (N0); N fertilizer applied at a rate of 380 kg N ha^{-1} (N380); and manure (cattle dung) applied at rate of 30 t ha^{-1} (C/N ratio of 20, nitrogen content of 0.28%, and a 25 kg N ha^{-1} seasonal increase in use) in addition to N fertilizer applied at a rate of 225 kg N ha^{-1} (MN250). These treatments were maintained throughout the entire year with three replications in 9 plots, which measured 8.0 m × 7.0 m each (with a buffer zone of 1.0 m between the plots), distributed in a completely randomized block design. After ridging the treatment plots, chemical fertilizer was applied to the soil in the form of 40% N (as urea: 46% N), 40 kg P ha^{-1} (as calcium super phosphate: 12% P_2O_5), and 80 kg K ha^{-1} (as potassium sulfate; 45% K_2O). Next, the soil was plowed to distribute the fertilizer into the subsurface, and prior to planting, manure was broadcast throughout the plots and buried in the soil with hoes. Using a hole-sowing machine in the furrows, 30% of the N fertilizer was applied at the jointing stage (June 21st, 2012 and June 30th, 2013), and the remaining 30% was applied at the silking stage (July 14th, 2012 and July 16th, 2013). In April of both years, the maize was sown at a depth of 5 cm and a density of 85,000 plants ha^{-1}, and it was harvested on September 8th, 2012 and September 12th, 2013. The soil water supply depended solely on natural rainfall.

2.3. Sample collection and measurements

2.3.1. Soil gases

The soil-air samplers used in each plot were multiport gas wells composed of poly-vinyl chloride (PVC) tubes with an inner diameter of 44 mm (Cates and Keeney, 1987; Wang et al., 2013). These sampling wells were composed of six gas chambers and were installed at depths of 7, 15, 30, 50, 70 and 90 cm (for more details, see Nan et al., 2015). Each gas chamber was connected to the soil surface via a tubule (4 mm in diameter), and twelve air holes were then drilled in the lower part of the chamber wall

(2 mm in diameter) and covered with nylon mesh. Each gas tubule, which was made of organic glass, was connected by a plastic three-way stopcock, and the system remained closed when not in use. A soil–air sampler was placed into pre-drilled holes, and gas samples were collected weekly from each chamber between 8:00 AM and 11:00 AM using 10-mL plastic syringes connected to the tubules via the three-way stopcocks at the surface. From April, 2012, to September, 2013, the CO_2 concentrations were measured concurrently from the ambient gas above the soil surface (0 cm) and at various soil depths. The CO_2 concentrations were measured by injecting 1-mL samples directly into a gas chromatograph (Agilent 7890A) equipped with a flame ionization detector (FID) along with a conversion furnace nickel catalyst for CO_2 analyses at 300 °C; samples were always measured within 24 h of each other on the same day.

2.3.2. Soil indexes

During gas sampling, the soil temperature was measured at depths of 7, 15, 30, 50, 70 and 90 cm using portable digital thermometers (JM624, Jinming Instrument Ltd., Tianjin, China). For convenience, we took the 7, 15, 30, 50, 70 and 90 cm depths as representing the 0–10, 10–20, 20–40, 40–60, 60–80 and 80–100 cm soil layers, respectively.

Soil samples were collected at various depths every week during the maize growing season (MS) and every 20 or 30 days (approximately) during the fallow season (FS). However, no soil samples were collected from December to February of the following year due to soil freezing. During the sampling period, three subsamples were randomly collected from between the maize rows using a 4-cm-diameter soil auger and then mixed into one sample for each plot. Next, the samples were oven-dried at 105 °C to a constant weight to determine the gravimetric soil water content, and the soil water-filled pore space (WFPS, %) was subsequently calculated. Finally, the soil bulk density was measured using a cutting-ring (a volume of up to 100 cm³). These data were collected every two weeks from the depths of 7, 15 and 30 cm, and the annual mean values of 1.43, 1.50 and 1.41 g cm⁻³ were used for the depths of 50, 70 and 90 cm in our calculations. Because the deviations from the measured means were small, they had less of an effect on our calculations than the variations in the soil WFPS.

Additional fresh soil samples were taken back to the laboratory and analyzed for water-soluble organic carbon (WSOC). Soil samples were treated with deionized water using 1:2 soil/water ratios (w/v) for 60 min under agitation (250 times min⁻¹) in a flask at 25 °C. After extraction, samples were centrifuged at 4000 r min⁻¹ for 20 min, and the supernatants were filtrated with a 0.45-μm Millipore membrane using a disposable syringe. The filtrate was analyzed through Pt-catalyzed, high-temperature combustion (680 °C) with a TOC-5050A analyzer (Shimadzu).

2.3.3. Plant biomass sample

Three adjacent plants in a row (at least 1 m from the plot edges and 0.5 m from previous sample sites) were randomly sampled from each plot at the sixth-leaf stage (V6, on June 2nd, 2012 and June 1st, 2013), tenth-leaf stage (V10, on June 20th, 2012 and June 15th, 2013), silking stage (R1, on July 13th, 2012 and July 14th, 2013), milk stage (R3, August 4th, 2012 and July 31st, 2013), ripe stage (R5, on August 24th, 2012 and August 21st, 2013) and at physiological maturity (R6, on September 7th, 2012 and September 16th, 2013), respectively. The harvested plants were killed by heating them at 105 °C for 30 min and weighed after oven-drying at 70 °C to a constant weight; the total above ground biomass in each plot was expressed in terms of kg dry matter ha⁻¹. At maturity, the grain yield was measured for all plants selected from a 10 m² area in each plot after being dried to a constant weight in a fan oven. All of the mass values are expressed in relation to the dry weight.

2.4. Calculations and statistical analyses

2.4.1. Soil water-filled pore space

The soil water-filled pore space (WFPS, %) was subsequently calculated using the following Eq. (1) (Linn and Doran, 1984):

$$\text{WFPS} = \frac{Ws \times \rho_b}{1 - (\rho_b/\rho_s)} \times 100\% \tag{1}$$

where Ws is the gravimetric soil water content (%); ρ_b is the dry bulk density (g m⁻³) at each soil depth; and ρ_s is the average particle density of soil (2.65 g m⁻³).

2.4.2. Efflux and production of CO_2 between soil layers

The basic method of our study followed that of Campbell (1985). It was assumed that the soil conditions are steady-state and uniform in horizontal direction, and it was also assumed that the gas diffusion in soil is an one-dimensional vertical flux (molecular diffusion within the air-filled pore space that fundamentally follows Fick's law as follows (Marshall, 1959; Rolston, 1986):

$$f = -D_p \frac{\partial C}{\partial Z} \tag{2}$$

where f is the CO_2 flux (g gas m⁻² soil s⁻¹); D_p is the soil gas diffusivity (m³ soil air m⁻¹ soil s⁻¹); C is the concentration of CO_2 in the air-filled pore space; Z is the distance between two soil layers; and $\partial C/\partial Z$ is the gradient of soil CO_2 concentration (g gas m⁻³ soil air m⁻¹ soil). If the gas transport upward, which defined the positive direction, and then inverse is the negative direction.

The gradient of flux at each depth can indicate the CO_2 production rate at that depth using the following Eq. (3) (Fierer et al., 2005; Hashimoto et al., 2007):

$$p_t = f_i - f_{i+1} \tag{3}$$

where P is the CO_2 production rate (g gas m⁻² soil s⁻¹); subscript i is a soil layer (cm); and subscript $i + 1$ is an adjacent i layer (cm). Note that the CO_2 production rate obtained in this study had the unit of flux.

The D_p is derived from the structure-dependent water induced-linear reduction (SWLR) model, which predicts the D_p/D_0 of soil depths, using the following Eq. (4) (Moldrup et al., 2013):

$$D_p = D_0 \varepsilon^{(1+C_m \Phi)} \left(\frac{\varepsilon}{\Phi} \right) \tag{4}$$

where D_0 is the gas diffusion coefficient in air (m³ air m⁻¹ air s⁻¹); ε is the soil air filled porosity (m³ air m³ soil); Φ is the soil porosity (m³ voids m³ soil); and C_m is the media complexity factor. Moldrup et al. (2013) compared many prediction models and recommended the SWLR model with a C_m value of 2.1 for intact soil. Fan and Jones (2014) demonstrated that the CO_2 concentration gradient in the soil profile is a reasonable estimator of CO_2 flux when measurements of the soil water content and known porosity values are used to estimate the gas diffusion coefficient.

The Millington–Quirk model was used to compute ε and Φ as follows (Millington and Quirk, 1961):

$$\Phi = 1 - \frac{\rho_b}{\rho_s} \tag{5}$$

$$\varepsilon = \Phi - \theta \tag{6}$$

where ρ_b is the dry bulk density (g m⁻³) at each soil layer; ρ_s is the average particle density of soil (2.65 g m⁻³); and θ is the volumetric soil water content at each depth.

The diffusion coefficient D_0 of CO_2 is affected by temperature and pressure and can be estimated as follows (Campbell 1985):

$$D_0 = D_{\text{stand}} \left(\frac{t + 273.15}{273.15} \right)^{1.75} \left(\frac{p_0}{p} \right) \qquad (7)$$

where D_{stand} is $1.39 \times 10^{-5}\,\text{m}^2\,\text{air}\,\text{s}^{-1}$ at 293.15 K and 1 kPa (Pritchard and Currie, 1982) for CO_2 gas diffusion coefficient in free air; t is the temperature (°C); and p is the pressure (hPa). Using the topographic elevations, $p_0 = 1013.3$ was calculated for China, and $p = 878.8$ was calculated for the Chanwu station.

2.4.3. Cumulative amount

The cumulative effluxes were obtained by multiplying the average efflux from two consecutive measurements within a week by the number of days between the measurements followed by summing the effluxes of these periods to a cumulative efflux for the period as follows (Wang et al., 2014):

$$T = \sum_{i=1}^{n} (X_i \times 24) \qquad (n = 1, 2, 3 \ldots) \qquad (8)$$

where T is cumulative effluxes (kg ha^{-1}); X is average daily CO_2 efflux rate ($\text{kg ha}^{-1}\,\text{h}^{-1}$); and i is the number of days. The calculation formula of cumulative production is similar to that for cumulative efflux (Eq. (8)). Thus, the production rate of these periods is summed for cumulative production.

The differences between the treatments were analyzed using a one-way analysis of variance (ANOVA) and were considered by t-test for least significant differences (LSD) at $P < 0.05$ or $P < 0.01$. Mean values, standard deviations, significance and correlations coefficients were estimated using SPSS16.0 (SPSS for Windows 10.0.1, SPSS Inc.) and an Excel spreadsheet (Microsoft Corp., USA).

3. Results

3.1. Soil physical indexes and nutrient concentrations

3.1.1. Soil temperature and soil water-filled pore space

Fertilizer application affected the soil temperature at each depth during the two years of the study (Table 1). In contrast to the N0 treatment, the mean temperatures within the N380 plots under the MS treatment were lower by 2.8, 1.5, 0.9, 1.1, 1.0 and 0.1 °C at the depths of 7, 15, 30, 50, 70 and 90 cm, respectively, and the MN250 plots were lower by 2.1, 1.2, 0.8, 0.5, 0.8 and 0.2 °C at 7, 15, 30, 50, 70 and 90 cm. The results indicated that fertilizer application substantially decreased soil profile temperature during the MS because fertilizer application can promote plant growth and improve vegetation coverage, resulting in decreased thermal radiation near the ground.

Table 1
Mean temperatures of each soil layer in different treatments (°C).

Soil depth	MS[a]			FS		
	N0[b]	N380	MN250	N0	N380	MN250
7 cm	22.4	19.7	20.3	6.9	6.5	7.9
15 cm	20.8	19.4	19.6	8.7	8.8	9.3
30 cm	20.0	19.1	19.3	9.8	10.3	11.0
50 cm	20.3	19.2	19.8	9.9	9.2	10.5
70 cm	20.5	19.5	19.6	10.1	8.9	10.0
90 cm	20.5	20.4	20.3	9.7	9.8	9.7

[a] MS and FS denote the maize growing season and fallow season, respectively. The date MS were from April 16th to September 8th, 2012, and were from April 16th to September 13th, 2013; the FS from September 9th, 2012 to April 15th, 2013. The average soil temperature is calculated by measuring the soil temperature at collecting gas samples.
[b] N0 denotes no N applied; N380, N applied at 380 kg N ha^{-1}; MN250, manure and N applied at 225 kg N ha^{-1}.

The soil water content for the two study years is shown in Fig. 1, and the results indicated that the fluctuation of the soil WFPS decreased with greater soil depth for all treatments. Rainfall events can increase the soil water contents at various depths, especially at the depths of 7 and 15 cm (Fig. 1b and c). The two-year mean for the WFPS of the N0 treatment (64.6%) was significantly higher than that of the N380 (58.8%) and MN250 (58.0%) treatments within the 0–100 cm soil ($P < 0.05$) with the WFPS mainly occurring at the depths of 7, 15 and 30 cm. Similar patterns were found throughout the entire MS, especially during the period of soil water stress (from early June to mid-July) in both years. The mean WFPS of the soil profiles was 55.4% (N0), 47.7% (N380) and 45.9% (MN250) during the period of soil water stress, when it reached its lowest point for the whole growth period due to less rainfall and increased absorption caused by rapid plant growth. The WFPS increased with additional rainfall, and during the FS, there were no differences in the WFPS values among all treatments at various depths.

3.1.2. CO_2 diffusion coefficient in the soil

The CO_2 diffusion coefficient (D_p) was calculated by the model (Eq. (4)), and it varied with farming practices and crop growth. There were three peaks for the D_p values in April (for plowing), June
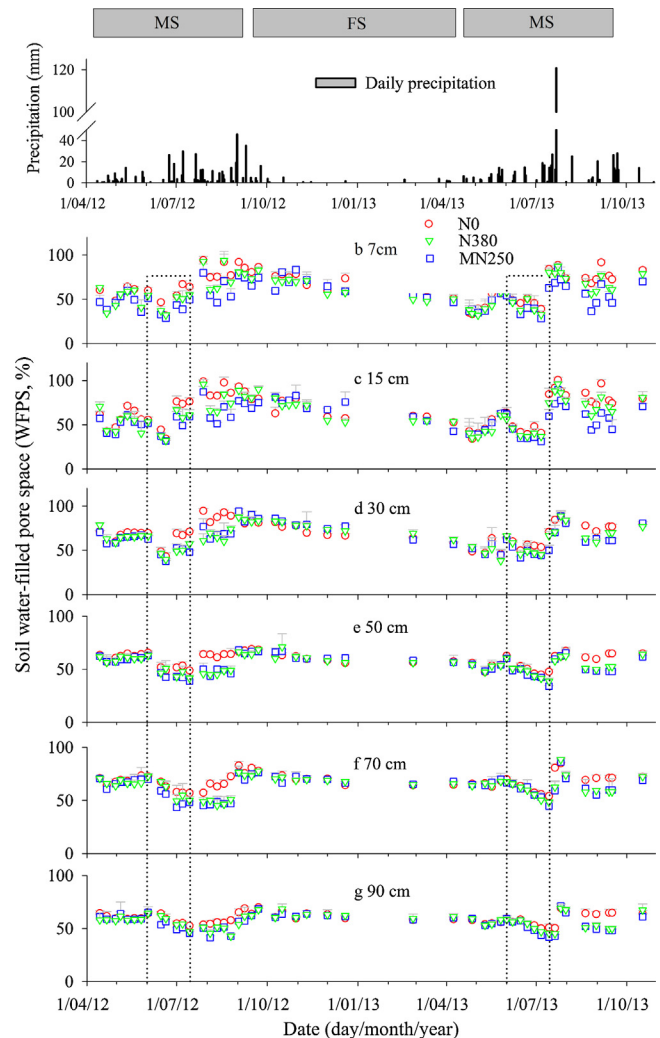

Fig. 1. Soil water-filled pore space (WFPS, %) of each layer in the different treatments. The bars represent the standard deviations of the means ($n = 3$), and MS and FS denote the maize growing season and fallow season. The N0 treatment denotes no N applied; N380: N applied at 380 kg N ha^{-1}; MN250: manure and N applied at 225 kg N ha^{-1}. Dotted boxes indicate the period of soil water stress.
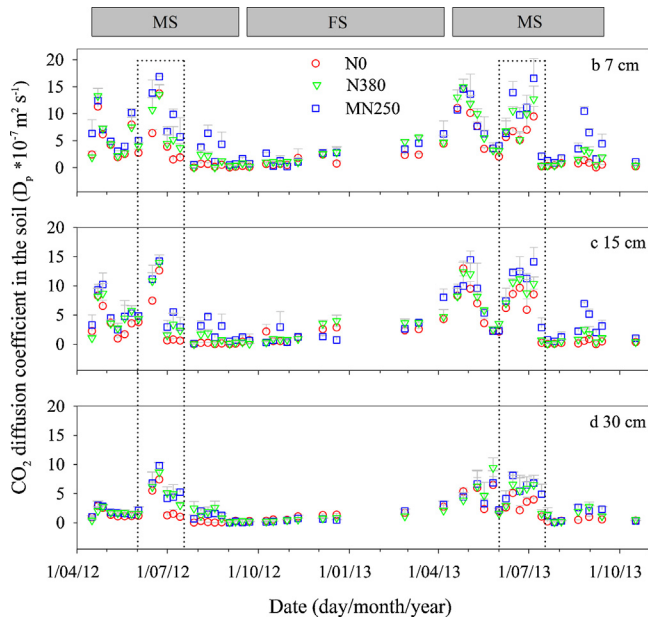
Fig. 2. CO_2 diffusion coefficients (D_p) in the soil layer above 40 cm in the different treatments. The bars represent the standard deviations of the means ($n = 3$), and the definitions of the codes for the seasons and treatments are shown in the footnote of Fig. 1. Dotted boxes denote the peak seasons for diffusion during the MS.

coefficient remarkably. Considering that a similar diffusion coefficient resulted from similar soil bulk density and soil WFPS values in deep soil, we did not present the D_p values for the 40–100-cm depths.

3.1.3. Soil water-soluble organic carbon

Soil WSOC contents were influence by fertilizer application, mainly at 7 and 15 cm depth (Fig. 3). The mean WSOC content for MN250 at 7 cm (82.1 mg kg^{-1}) was significantly higher than that of the N0 (57.0 mg kg^{-1}) and N380 (45.1 mg kg^{-1}) treatments during the study period (Fig. 3b and c), and a similar pattern appeared at 15 cm, for which the mean values were 58.0 mg kg^{-1} (MN250), 55.3 mg kg^{-1} (N0) and 40.7 mg kg^{-1} (N380). Among all of the treatments, there were no differences below 30 cm, and the mean WSOC values for the MN250, N0 and N380 treatments were 34.9, 33.0 and 31.5 mg kg^{-1}, respectively (Fig. 3d–g). The results revealed that the application of organic matter significantly increased the WSOC contents of the soil, but N application decreased soil WSOC contents, mainly in the surface soil.

3.2. Dry matter accumulation and grain yield

Fertilizer application increased both the amount of dry matter over the entire growing season and the grain yield (Table 2). In contrast with the N0 treatments, the after-harvest dry matter in the N380 and MN250 treatments increased by 140.8% and 146.9%, respectively, in 2012 and by 214.8% and 301.1% in 2013. No significant difference in dry matter accumulation was observed in any sampling stage between the N380 and MN250 treatments. During the R5 to R6 maize stages, dry matter accumulation did not increase in the N0 treatment, but the values in the fertilization treatments continued to increase, which indicated that fertilization extended the growth period of the crop. The grain yields under the N380 and MN250 treatments were all significantly higher than under the N0 treatment, by 193.9% and 210.2%, respectively, in 2012 and 400.0% and 458.6% in 2013. The difference in grain yield
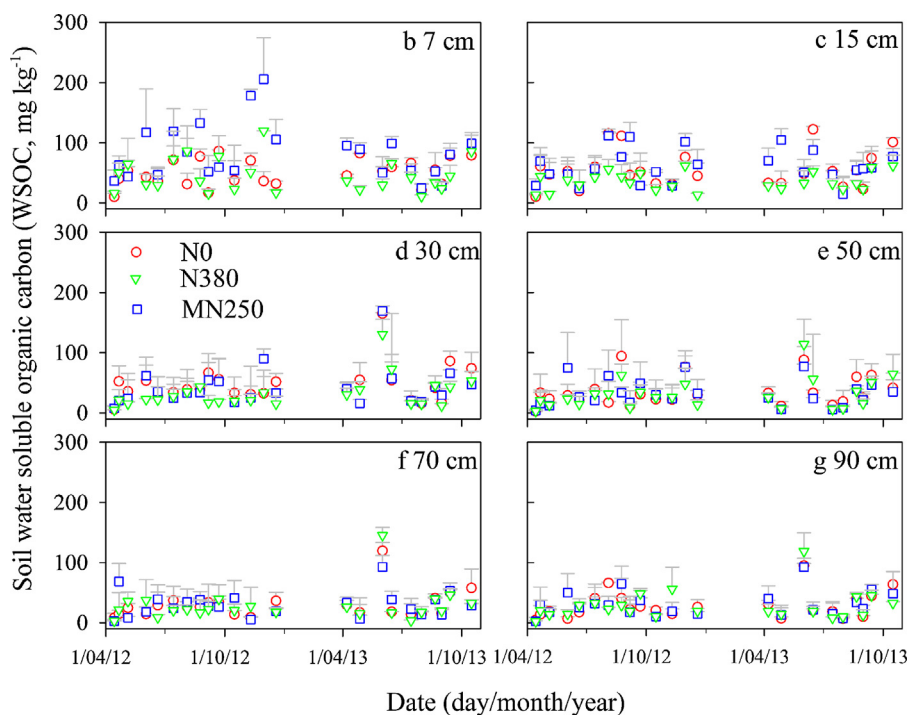
and September (Fig. 2), and the soil values decreased with depth and varied with season because soil air porosity was determined from soil bulk density and soil water content. The mean diffusion coefficient between the atmosphere and the topsoil in the N0 treatment (3.3×10^{-7} m^2 s^{-1}) was slightly lower than that of the N380 treatment (4.3×10^{-7} m^2 s^{-1}) and significantly lower than that of MN250 treatment (6.3×10^{-7} m^2 s^{-1}). This demonstrated that manure application can increase the gas-diffusion

Fig. 3. Soil water-soluble organic carbon (WSOC) of each soil layer under different treatments. The bars represent the standard deviations of the means ($n = 3$), and the definitions of the codes for the treatments are shown in the footnote to Fig. 1.

Table 2
Dry matter accumulation of growth stage and grain yield (Mg ha^{-1}).

Growth stage	2012			2013		
	N0[a]	N380	MN250	N0	N380	MN250
V6[b]	0.3 ± 0.1a[c]	0.5 ± 0.0a	0.8 ± 0.1a	0.3 ± 0.1a	0.3 ± 0.1a	0.4 ± 0.0a
V10	3.2 ± 0.1b	4.8 ± 0.3ab	5.8 ± 0.2a	2.9 ± 0.9a	4.3 ± 0.9a	5.0 ± 0.4a
R1	6.6 ± 0.3b	10.8 ± 1.4a	11.8 ± 0.8a	8.4 ± 1.4b	12.0 ± 1.3ab	12.7 ± 0.8a
R3	7.3 ± 2.2b	15.1 ± 1.4a	16.9 ± 1.3a	9.8 ± 1.6b	14.7 ± 0.6a	18.3 ± 0.2a
R5	9.8 ± 1.4b	19.4 ± 1.9a	20.4 ± 1.4a	9.8 ± 2.4b	19.2 ± 1.2a	22.3 ± 3.8a
R6	9.8 ± 2.4b	23.6 ± 0.6a	24.2 ± 0.8a	8.8 ± 3.3c	22.8 ± 0.2b	25.8 ± 0.9a
Grain yield	4.9 ± 1.4b	14.4 ± 0.6a	15.2 ± 0.6a	2.9 ± 0.4c	14.5 ± 0.3b	16.2 ± 0.3a

[a] Definitions of the treatment codes are shown in the footnotes of Table 1.
[b] The letter represents the maize growth period of sixth-leaf stage (V6), tenth-leaf stage (V10), silking stage (R1), milk stage (R3), ripe stage (R5), and physiological maturity (R6).
[c] Values are expressed as the mean ± deviation (n = 3). The values within the rows with different letters are significantly different at $P < 0.05$.

between the N380 and MN250 treatments was not obvious in 2012 but significant in 2013.

3.3. Soil profile CO_2

3.3.1. CO_2 distribution

The CO_2 concentrations showed strong seasonal variations, and they significantly increased within the 0–50-cm layer and then remained constant (Fig. 4). During the MS, the mean CO_2
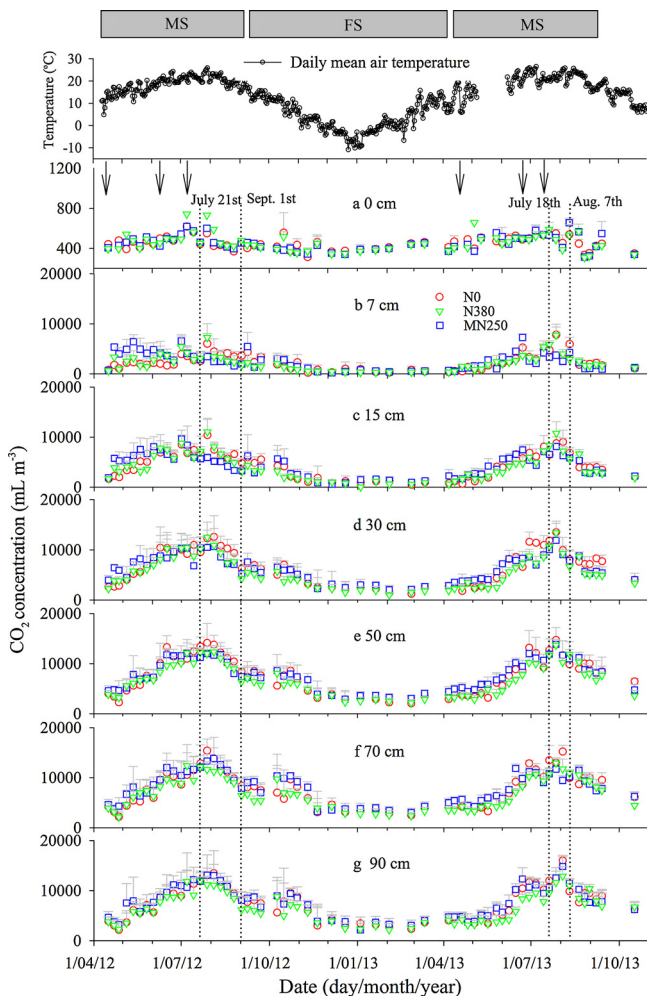

Fig. 4. CO_2 concentrations of each soil layer under different treatments. The bars represent the standard deviations of the means (n = 3), and the solid arrows denote the dates of fertilizer application. Dotted lines denote heavy rainfall events, and the definitions of the codes for the seasons and treatments are shown in the footnote of Fig. 1.

concentrations for the 0–100-cm layer in the MN250 (6639 mL m^{-3}) and the N0 (6505 mL m^{-3}) treatments were significantly higher than that of the N380 (5952 mL m^{-3}) treatment ($P < 0.05$). The pattern was primarily observed at the depths of 7 and 15 cm, especially from April 16th to July 14th (Fig. 4b and c), but there were no significant differences throughout the soil profiles among N0, N380 and MN250 during the FS. The CO_2 concentrations in the entire soil profile responded rapidly to heavy precipitation events and synchronously decreased after heavy rainfall events (27.4 mm on July 21st, 2012; 46.0 mm on September 1st, 2012; 27.0 mm on July 18th, 2013; and 25.2 mm on August 7th, 2013) and extraordinary rainfall events (120.8 mm on July 22nd, 2013).

3.3.2. CO_2 effluxes

The CO_2 efflux rates significantly decreased with increasing soil depth and showed stronger trends from early June to mid-July (Fig. 5). In the surface soil, the CO_2 efflux rates rapidly increased by 4–8 times after plowing, declined, and then gradually increased (Fig. 5a and b). The mean efflux rate for the 0–100-cm layer in the MN250 treatment (41.8 mg CO_2 m^{-2} h^{-1}) was significantly higher than those of the N380 treatment (28.5 mg CO_2 m^{-2} h^{-1}) and the N0 treatment (22.0 mg CO_2 m^{-2} h^{-1}) during the MS ($P < 0.05$). The mean efflux rates during the MS of the two years were as follows for the depths of 7, 15 and 30 cm, respectively: 167.5, 90.4 and 27.1 mg CO_2 m^{-2} h^{-1} for the MN250 treatment; 100.1, 75.0 and 23.9 mg CO_2 m^{-2} h^{-1} for the N380 treatment; and 69.7, 62.9 and 17.6 mg CO_2 m^{-2} h^{-1} for the N0 treatment. The mean efflux rates among the various treatments remained low below 30 cm in depth during the MS and at all soil depths during the FS.

Fertilizer addition increased the cumulative CO_2 effluxes, especially in the surface soil. During the MS, the cumulative effluxes for the MN250 treatment (6418.4 kg CO_2 ha^{-1} and 3323.0 kg CO_2 ha^{-1}) at 7 cm and 15 cm were significantly higher than those of the N380 (3920.0 kg CO_2 ha^{-1} and 2707.9 kg CO_2 ha^{-1}) and N0 (2886.9 kg CO_2 ha^{-1} and 2006.4 kg CO_2 ha^{-1}) treatments during the MS ($P < 0.05$) (Fig. 6A). During the FS, the cumulative CO_2 effluxes of the MN250 treatment were significantly higher than those of the N380 and N0 treatments, but no difference was observed between the N380 and N0 treatments (Fig. 6B). Regardless of season (MS or FS), the mean cumulative effluxes below 50 cm were low or even negative. The cumulative CO_2 effluxes in the surface soil for the whole year (8312.4 kg CO_2 ha^{-1}) accounted for 76.3% of the total effluxes within the soil profile (10,888.2 kg CO_2 ha^{-1}), thus demonstrating that abundant CO_2 effluxes occurred in the surface soil (0–15 cm) during the MS.

3.3.3. CO_2 production

Based on Eq. (3), we calculated the CO_2 production rate between soil layers by the inversion method. There was a high production rate at the depths of 7 cm (43.2 mg CO_2 m^{-2} h^{-1}) and 15 cm
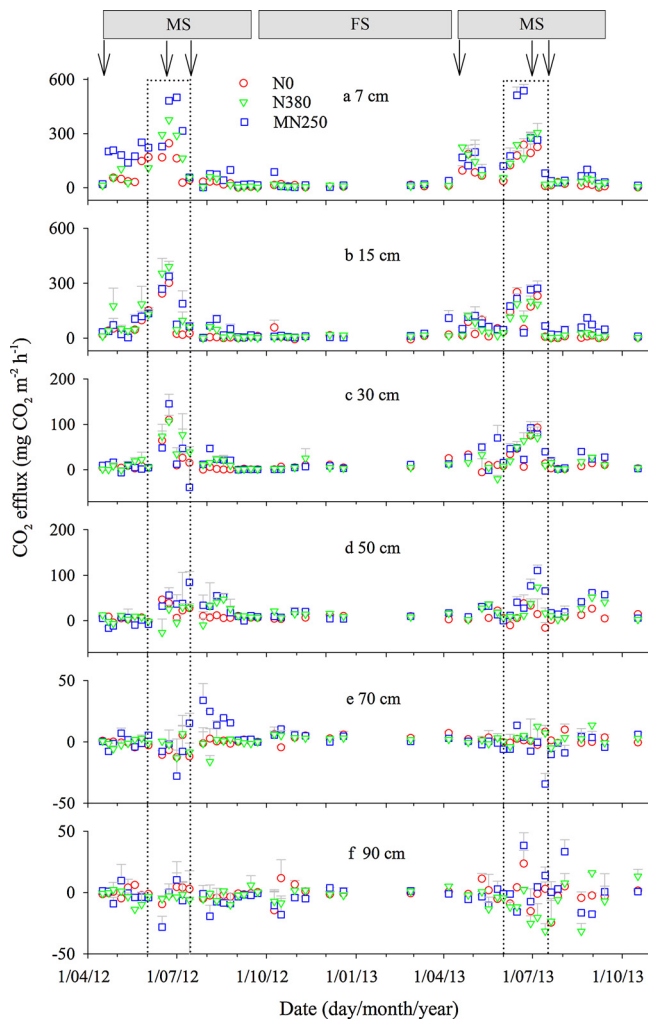
Fig. 5. CO_2 effluxes of each soil layer under different treatments. The bars represent the standard deviations of the means ($n = 3$), and solid arrows denote the dates of fertilizer application. Dotted boxes indicate the peak seasons of effluxes, and the definitions of the codes for the seasons and treatments are shown in the footnote of Fig. 1.

(40.1 mg CO_2 m^{-2} h^{-1}) and low production rates in deep soil (Fig. 7). However, the production rate at 30 cm (4.7 mg CO_2 m^{-2} h^{-1}) was lower than that at 50 cm (16.8 mg CO_2 m^{-2} h^{-1}), so the mean production rate for the 0–100 cm layer in the MN250 treatment (114.6 mg CO_2 m^{-2} h^{-1}) was greater than those in the N380 (76.4 mg CO_2 m^{-2} h^{-1}) and N0 (54.2 mg CO_2 m^{-2} h^{-1}) treatments during the MS ($P < 0.01$).

Undoubtedly, the addition of fertilizer also significantly increased the cumulative production of CO_2, especially at the soil depth of 15 cm, during the MS (Table 3). The cumulative production of CO_2 in the MN250 treatment (3173.9 kg CO_2 ha^{-1} for 7 cm and 2180.7 kg CO_2 ha^{-1} for 15 cm) was significantly higher than that in the N380 (1386.3 kg CO_2 ha^{-1} for 7 cm and 1803.9 kg CO_2 ha^{-1} for 15 cm) and N0 (855.9 kg CO_2 ha^{-1} for 7 cm and 1274.3 kg CO_2 ha^{-1} for 15 cm) treatments during the MS ($P < 0.05$). The data clearly indicated that manure application significantly increased CO_2 production. During the MS, the productive contribution rate of CO_2 at the depth of 15 cm was higher than that at 7 cm in the N0 and N380 treatments, but the opposite trend occurred in the N250 treatment (Table 3). These results implied that abundant soil CO_2 production occurred at 15 cm, but manure addition significantly improved the productive contribution rate of the surface soil. During the FS, the mean amount of CO_2 production for all treatments at the depths of 7 and 30 cm were negative, −146.3 and −197.0 kg CO_2 ha^{-1}, respectively.

4. Relationship between CO_2 and soil variables

In all treatments, a significant relationship was found between CO_2 concentrations and temperature at each soil depth (Table 4). There was a significant positive correlation between CO_2 concentrations and soil WFPS from 0 to 20 cm in depth and a significant negative correlation from 40 to 100 cm in depth. Nevertheless, there was a significant negative correlation between CO_2 concentrations and the diffusion coefficient from 0 to 20 cm and a significant positive correlation from 40 to 100 cm in the soil (Table 4), which was attributed to more rapid production and efflux of soil CO_2 from 0 to 20 cm. In addition, we found a negative correlation between CO_2 concentrations and soil WSOC contents at each depth.
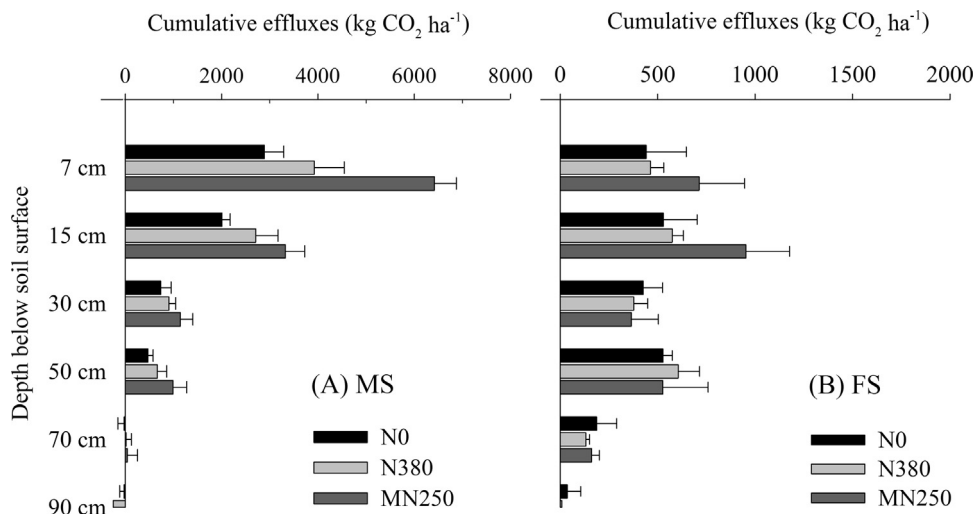

Fig. 6. Cumulative CO_2 effluxes of each soil layer under different treatments. The bars represent the standard deviations of the means ($n = 6$ for MS, $n = 3$ for FS). Definitions of the codes for the seasons and treatments are shown in the footnote of Fig. 1.
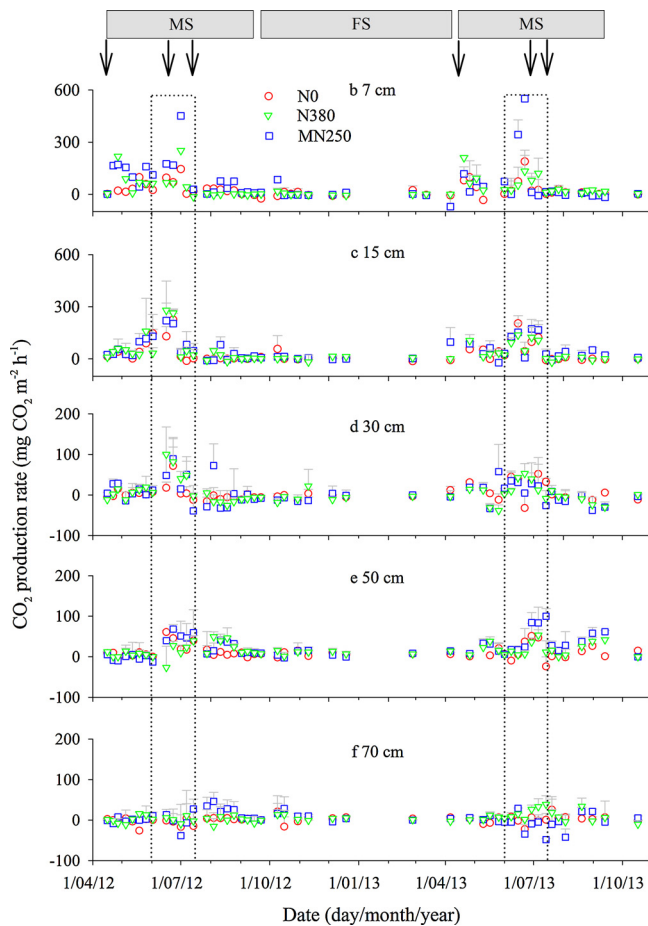
Fig. 7. CO_2 production rates of each soil layer under different treatments. The bars represent the standard deviations of the means ($n = 3$). Definitions of the codes for the seasons and treatments are shown in the footnote of Fig. 1.

5. Discussion

5.1. Variation of CO_2 in the soil profile

In all of the soil profiles, CO_2 concentrations increased with increasing soil depth (Fig. 4), but CO_2 effluxes and production decreased with increasing soil depth (Figs. 5 and 7), which was correlation with gas diffusion and production. In the surface soil, higher production rates, together with higher diffusion, led to lower soil CO_2 concentrations, but there were lower production effluxes combined with lower gas diffusion at greater depths, which led to higher soil CO_2 concentrations. In addition, CO_2 effluxes and production in the soil profile have distinctive variations related to gas diffusion and root-derived C inputs to the soil (Hashimoto and Komatsu 2006; Iversen et al., 2012), which were much larger in the surface than in the subsurface soil (Fig. 6 and Table 3). These variations could also be explained by the decrease in soil WSOC content with increasing soil depth. The cumulative CO_2 effluxes in the surface soil for the whole year accounted for 76.3% of the total effluxes of the soil profile, so the surface soil effluxes were abundant. These results agree with the results of other studies (Davidson and Trumbore, 1995; Fierer et al., 2005; Hashimoto and Komatsu 2006; Koehler et al., 2012; Moncrieff and Fang 1999). We also noted that the CO_2 concentrations in each layer increased with increasing soil temperature (Table 4), which is also consistent with previous research (Bajracharya et al., 2000; Epron et al., 1999; Fang and Moncrieff, 2001). Based on the relationship between CO_2 contents and soil variables, we inferred that the physical soil conditions and nutrient status were likely to play an important role in soil CO_2 production and effluxes over the long term.

5.2. Soil CO_2 and fertilization

Fertilization could alter physical soil conditions and nutrient status, such as by promoting gas diffusivity, decreasing soil temperature and soil WFPS content, and transforming C (Ramirez et al., 2010; Xu et al., 2011). Compared with the N0 treatment, the high addition of N (N380) increased the amount of dry matter over the entire growing season as well as the grain yield (14.5 Mg ha^{-1}, Table 3); it also promoted soil effluxes and the production of CO_2 through stronger respiration (Figs. 6 and 7). Some studies have reported that N application decreases soil CO_2 production (due to organic carbon limitation) (Liu and Greaver, 2009; Mosier et al., 2003) or increases CO_2 effluxes (priming effect of N fertilizer) (Brumme and Beese, 1992), but our study confirmed that N addition, which may be predominantly root-driven, could accelerate CO_2 production in the soil profile of an agro-ecosystem.

In contrast to the N0 and N380 treatments, the integrated application of manure and N (MN250) significantly increased gas diffusion and crop growth (Fig. 2 and Table 2) as well as improved effluxes and production of CO_2 in the soil profile. Therefore, the productive contribution rate in the surface soil increased, which was related to manure. Cumulative CO_2 production in the topsoil during the MS slightly increased by 530.4 kg CO_2 ha^{-1} in the high-N treatment (N380) compared with that in the N0 treatment, but the cumulative production in the MN250 treatment increased by 2487.1 kg CO_2 ha^{-1} compared with that in the N0 treatment and by 1951.3 kg CO_2 ha^{-1} compared with the N380 treatment (Table 3). Despite the effect of the extra 130 kg N ha^{-1} N (the difference between 380 and 250 kg N ha^{-1}), our data demonstrated that incremental increase in CO_2 production from the application of manure was almost four times higher than the increase from the application of N fertilizer. This can be explained by the application of cattle manure in the topsoil, which can provide abundant

Table 3
Seasonal cumulative CO_2 production and contribution rates of each soil layer in different treatments (kg CO_2 ha^{-1}).

Soil depth	MS[a]			FS			Contribution rate of the MS (%)[d]		
	N0[b]	N380	MN250	N0	N380	MN250	N0	N380	MN250
7 cm	855.9 ± 364.4c[c]	1386.3 ± 157.9b	3337.6 ± 496.0a	−88 ± 286.4a	−111.5 ± 123.6ab	−239.5 ± 159.2c	29.6	31.6	47.9
15 cm	1274.3 ± 258.4c	1803.9 ± 474.7b	2180.7 ± 329.8a	103 ± 145.9c	297.4 ± 96.7ab	587.2 ± 360.0a	44.1	41.1	32.9
30 cm	262.5 ± 246.2ab	285.2 ± 259.6a	155.0 ± 310.6bc	−101 ± 52.2a	−328.7 ± 71.1c	−161.3 ± 337.3ab	9.1	6.5	2.3
50 cm	496.7 ± 175.7a	646.3 ± 116.0a	945.7 ± 449.6a	340 ± 145.3a	474.4 ± 117.4a	365.3 ± 270.4a	17.2	14.7	14.3
70 cm	2.0 ± 172.9a	269.8 ± 245.9a	169.4 ± 256.7a	151 ± 135.4a	122.5 ± 26.6a	212.3 ± 85.6a	0.1	6.1	2.6

[a] Definitions of the codes for the seasons are shown in the footnotes of Table 1.
[b] Definitions of the codes for the treatments are shown in the footnotes of Table 1.
[c] Mean values (mean ± standard deviation, $n = 6$ for MS, $n = 3$ for FS) within the same row followed by the different letters are significantly different at $P < 0.05$.
[d] Contribution rate in each soil layer is contribution to whole profile CO_2 production (% of total).

Table 4
Pearson correlation coefficients (r) between the CO_2 concentrations (ml m^{-3}) and soil variables in each soil layer.

Soil depth	Temperature (°C)		Soil WFPS (%)		D_P (m^2 s^{-1})		WSOC (mg kg^{-1})	
	n[a]	r[b]	n	r	n	r	n	r
7 cm	186	0.63***[c]	162	0.18*	162	−0.05	72	−0.18
1 cm	186	0.77***	162	0.20*	162	−0.08	68	−0.05
30 cm	186	0.75***	144	0.05	144	0.04	72	−0.11
50 cm	186	0.78***	144	−0.31***	144	0.38***	72	−0.05
70 cm	186	0.74***	144	−0.23**	144	0.43***	72	−0.14
90 cm	186	0.71***	144	−0.30***	127	0.37***	72	−0.08

[a] n, number of observation.
[b] r, pearson correlation coefficient, 2-tailed tests of significance.
[c] *significant at $P < 0.05$; **significant at $P < 0.01$; ***significant at $P < 0.001$.

organic carbon and promote microbial CO_2 production. As is well known, soil WSOC, which is derived from the higher decomposition rate of the organic carbon, is an important source of active organic carbon and is directly related to the CO_2 content of the soil profile (Hassan et al., 2014; Ping et al., 2001; Williams and Edwards, 2006). Neff and Hooper (2002) and Kane et al. (2006) suggested that the soil WSOC concentrations may increase as the microbial processing activities within soils increase, and in this study, the soil WSOC content of the MN250 treatment (82.1 mg kg^{-1}) was significantly higher than those of the N0 (57.0 mg kg^{-1}) and N380 treatments (45.1 mg kg^{-1}) (Fig. 3), which implied that the mineralization in the MN250 treatment remained high throughout the observation period (Kane et al., 2006; Neff and Hooper, 2002). Therefore, microbial respiration could explain why so much CO_2 production was observed in the topsoil and why the addition of manure could enhance topsoil CO_2 production. Nevertheless, manure decreased the productive contribution rate from 10 to 20 cm in depth, which might be attributed to the relatively increased production.

5.3. Soil CO_2 and crop growth

The period from June to mid-July happens to be the V6 to R1 maize growth stage, which is a time of rapid root growth (Bu et al., 2013; Liu et al., 2014a, (at the same site); Hu et al., 2009), and it is the time that CO_2 production and efflux sharply increases with increasing gas diffusion (Figs. 4 and 8) as well as decreasing soil WFPS (Fig. 2). During this period, cumulative effluxes and cumulative production accounted for 52–57% and 64–76% of the annual values, respectively, so apparently, the asymmetry in the full range of CO_2 production primarily arises from substantial root growth (Zhuang et al., 2001). Unfortunately, however, there was a lack of root biomass during the maize growth period in our study, but Huang et al. (2007) and Kuchenbuch and Jung (1988) reported the root/shoot ratio of maize to be 0.09 or 0.15. Thus, we can infer the relationship between dry biomass and CO_2 production in our study; we reported that the cumulative production of CO_2 (within a depth of 40 cm) and dry matter during the V6, V10, R1, R3, R5 and R6 growing stages was significantly linearly correlated with correlation coefficients (R^2) of 0.83, 0.59, 0.41, 0.62, 0.29 and 0.36, respectively. The results confirmed that root respiration greatly influenced the CO_2 production of the soil profile, and the CO_2 concentration remained high even after plant growth ceased (it required a month to come down). These results were consistent with those of others (Hassan et al., 2014; Shi et al., 2014; Vargas et al., 2014), suggesting that the high CO_2 concentration was due to an abundance of crop residues being decomposed under higher temperature and moisture.

5.4. Underestimation of the model

The model assumed that all CO_2 transportation through the profile was by molecular diffusion, and it did not account for convective movement and the amount of CO_2 dissolved in the soil water, which leads to an underestimation of CO_2 efflux, as suggested by precious researchers (Fierer et al., 2005; Jassal et al., 2004). In addition, we used weekly average effluxes and so could not discern the short-term dynamics of soil CO_2 production following concentrated rainfall events, which also resulted in the underestimation of the cumulative amounts, which was consistent with previous research (DeSutter et al., 2008; Fan and Jones, 2014; Kusa et al., 2010). For example, during the MS, the CO_2 production rate drastically decreased in the post-silking stage (July 14th), which may be related to methodology or rainfall events. However, during the FS, the average soil temperatures were less than 10 °C, so the lower production rate and negative production of CO_2 at 7 cm might have been due to the sampling method or the downward movement of gas (Table 3). Apart from the preceding reasons, this underestimation might be attributed to the inaccurate measurement of soil moisture and soil bulk density under low temperatures, thereby resulting in an underestimation of the diffusion coefficient or even a determination of negative production. Moreover, a large amount of CO_2 sealed by frozen water in a low-temperature environment could also lead to negative production, but at the depth of 30 cm (plough pan), lower CO_2 production was observed throughout the study period, which may be related to porosity and bulk density. A maximum soil bulk density value was observed at the depth of 30 cm (average mean of 1.52 g cm^{-3}) as if the plough pan, which is more heavily compacted, was not conducive to the upward movement of gas from deep soil.

Despite the disadvantages presented in this paper, the study is among the few on fertilizer input management in the Loess Plateau region because much of the information about high-yield systems has been largely described. Therefore, more attention was focused on the relative rather than absolute GHG responses to the treatments and budgets. According to our results, the cumulative effluxes and production of CO_2 can better reveal the influence of regular fertilization on plants. The inferred cumulative CO_2 effluxes at the soil-atmosphere interface (Fig. 6) were consistent with other studies (Kim et al., 2007; Wu et al., 2010), but they were relatively higher compared with the value reported by Wang et al. (2014). As is well known, CO_2 production is not only influenced by physical soil conditions but also by the biochemical status, and it was rather difficult to single out the impacts of specific factors in the field. Nevertheless, the dominant factors, such as fertilization and root growth, have already been described. In addition, fertilization management, such as the depth of application, could affect CO_2 production. Future studies of CO_2 effluxes and production should attempt to distinguish between root respiration and soil microbial respiration within soil profiles.

6. Conclusion

Fertilizer application and crop growth triggered the production and transport of soil CO_2. Fertilizer application changes the physical conditions (temperature, moisture and gas diffusivity) of soil profiles to extend the crop growth period and accelerate CO_2 production in the soil, which mainly occurs during the maize growth season. In addition, a higher efflux rate was observed with a higher production rate from the sixth-leaf stage (V6) to the silking stage (R1) combined with the rapid diffusion of CO_2, while cumulative production and cumulative effluxes accounted for 64–76% and 52–57% of annual totals, respectively. Higher production and effluxes occurred in the surface soil, which, respectively, contributed 72.3% and 76.3% of the total amount of

CO_2 from 0 to 100 cm in soil depth. Higher N application (N380) increased the production and effluxes of CO_2 in the soil profile, but it did not affect the productive contribution rate of soil CO_2 at each depth. The integrated application of manure and nitrogen fertilizer (MN250) significantly increased the effluxes and production of soil CO_2. The addition of manure promoted greater soil CO_2 production than the contribution of N fertilizer alone.

Acknowledgements

References

Allen, M.R., Frame, D.J., Huntingford, C., Jones, C.D., Lowe, J.A., Meinshausen, M., Meinshausen, N., 2009. Warming caused by cumulative carbon emissions towards the trillionth tonne. Nature 458, 1163–1166.

Bajracharya, R.M., Lal, R., Kimble, J.M., 2000. Erosion effect on carbon dioxide concentration and carbon flux from an Ohio Alfisol. Soil Sci. Soc. Am. J. 64, 694–700.

Bond-Lamberty, B., Thomson, A., 2010. Temperature-associated increases in the global soil respiration record. Nature 464 (7288), 579–582.

Bowden, W.B., Bormann, F.H., 1986. Transport and loss of nitrous oxide in soil water after forest cutting. Science 233, 867–869.

Brumme, R., Beese, F., 1992. Effects of liming and nitrogen fertilization on emissions of CO_2 and N_2O from a temperate forest. J. Geophys. Res. 97 (12), 12851–12858.

Bu, L.D., Liu, J.L., Zhu, L., Luo, S.S., Chen, X.P., Li, S.Q., Hill, R.L., Zhao, Y., 2013. The effects of mulching on maize growth, yield and water use in a semi-arid region. Agric. Water Manage. 71–78.

Campbell, G.S., 1985. Soil physics with BASIC. Soil Science Society of America Book Series: 5 Methods of Soil Analysis Part I-Physical and Mineralogical Methods. Elsevier Science Publishers BV, Amsterdam.

Cates, R.L., Keeney, D.R., 1987. Nitrous oxide production throughout the year from fertilized and manured maize fields. J. Environ. Qual. 16, 443–447.

Chen, X.P., Cui, Z.L., Fan, M.S., Vitousek, P., Zhao, M., Ma, W.Q., Wang, Z.L., Zhang, W.J., Yan, X.Y., Yang, J.C., Deng, X.P., Gao, Q., Zhang, Q., Guo, S.W., Ren, J., Li, S.Q., Ye, Y.L., Wang, Z.H., Huang, J.L., Tang, Q.Y., Sun, Y.X., Peng, X.L., Zhang, J.W., He, M.R., Zhu, Y.J., Xue, J.Q., Wang, G.L., Wu, L., An, N., Wu, L.Q., Ma, L., Zhang, W.F., Zhang, F.S., 2014. Producing more grain with lower environmental costs. Nature 514 (7523), 486–489.

Cook, F.J., Thomas, S.M., Kelliher, F.M., Whitehead, D., 1998. A model of one-dimensional steady-state carbon dioxide diffusion from soil. Ecol. Model. 109, 155–164.

Davidson, E., Belk, E., Boone, R.D., 1998. Soil water content and temperature as independent or confounded factors controlling soil respiration in a temperate mixed hardwood forest. Global Change Biol. 4, 217–227.

Davidson, E.A., Janssens, I.A., 2006. Temperature sensitivity of soil carbon decomposition and feedbacks to climate change. Nature 440, 165–173.

Davidson, E.A., Savage, K.E., Trumbore, S.E., Borken, W., 2006. Vertical partitioning of CO_2 production within a temperate forest soil. Global Change Biol. 12 (6), 944–956.

Davidson, E.A., Trumbore, S.E., 1995. Gas diffusivity and production of CO_2 in deep soils of the eastern Amazon. Tellus B 47, 550–565.

Davidson, E.A., Verchot, L.V., Cattânio, J.H., Ackerman, I.L., Carvalho, J.E.M., 2000. Effects of soil water content on soil respiration in forests and cattle pastures of eastern Amazonia. Biogeochemistry 48, 53–69.

DeSutter, T.M., Sauer, T.J., Parkin, T.B., Heitman, J.L., 2008. A subsurface, closed-loop system for soil carbon dioxide and its application to the gradient efflux approach. Soil Sci. Soc. Am. J. 72, 126–134.

Elhottová, D., Koubová, A., Šimek, M., Cajthaml, T., Jirout, J., Esperschuetz, J., Schloter, M., Gattinger, A., 2012. Changes in soil microbial communities as affected by intensive cattle husbandry. Appl. Soil Ecol. 58, 56–65.

Epron, D., Farque, L., Lucot, É., Badot, P.M., 1999. Soil CO_2 efflux in a beech forest: dependence on soil temperature and soil water content. Ann. For. Sci. 56, 221–226.

Fan, J., Jones, S.B., 2014. Soil surface wetting effects on gradient-based estimates of soil carbon dioxide efflux. Vadose Zone J. 13 (2), 53–63.

Fang, C., Moncrieff, J.B., 2001. The dependence of soil CO_2 efflux on temperature. Soil Biol. Biochem. 33, 155–165.

Fang, Y.T., Gundersen, P., Zhang, W., Zhou, G.Y., Christiansen, J.R., 2009. Soil atmosphere exchange of N_2O, CO_2 and CH_4 along a slope of an evergreen broad-leaved forest in southern China. Plant Soil 319, 37–48.

Fierer, N., Chadwick, O.A., Trumbore, S.E., 2005. Production of CO_2 in soil profiles of a California annual grassland. Ecosystems 8, 412–429.

Gaudinski, J.B., Trumbore, S.E., Davidson, E.A., Zheng, S., 2000. Soil carbon cycling in a temperate forest: radiocarbon-based estimates of residence times, sequestration rates and partitioning of fluxes. Biogeochemistry 51, 33–69.

Gaumont-Guay, D., Black, T.A., Griffis, T.J., Barr, A.G., Jassal, R.S., Nesic, Z., 2006. Interpreting the dependence of soil respiration on soil temperature and water content in a boreal aspen stand. Agric. For. Meteorol. 140, 220–235.

Pedogenesis and Soil Taxonomy. In: Gong, Z.T., Zhang, G.L., Chen, Z.C. (Eds.), Bejing Science Press Publishing in Chinese.

Hashimoto, S., Komatsu, H., 2006. Relationships between soil CO_2 concentration and CO_2 production, temperature, water content, and gas diffusivity: implications for field studies through sensitivity analyses. J. For. Res. 11 (1), 41–50.

Hashimoto, S., Tanaka, N., Kume, T., Yoshifuji, N., Hotta, N., Tanaka, K., Suzuki, M., 2007. Seasonality of vertically partitioned soil CO_2 production in temperate and tropical forest. J. For. Res. 12, 209–221.

Hassan, W., David, J., Abbas, F., 2014. Effect of type and quality of two contrasting plant residues on CO_2 emission potential of Ultisol soil: implications for indirect influence of temperature and moisture. Catena 114, 90–96.

Hendry, M.J., Mendoza, C.A., Kirkland, R.A., Lawrence, J.R., 1999. Quantification of transient CO_2 production in a sandy unsaturated zone. Water Resour. Res 35, 2189–2198.

Hu, T., Kang, S.Z., Li, F.S., Zhang, J.H., 2009. Effects of partial root-zone irrigation on the nitrogen absorption and utilization of maize. Agric. Water Manage. 96 (2), 208–214.

Huang, Y., Zhang, W., Sun, W.J., Zheng, X.H., 2007. Net primary production of Chinese croplands from 1950 to 1999. Ecol. Appl. 17, 692–701.

Hynšt, J., Šimek, M., Brůček, P., Petersen, S.O., 2007. High fluxes but different patterns of nitrous oxide and carbon dioxide emissions from soil in a cattle overwintering area. Agric. Ecosyst. Environ. 120, 269–279.

Iversen, C.M., Keller Jr., J.K., C.T.G, Norby, R.J., 2012. Soil carbon and nitrogen cycling and storage throughout the soil profile in a sweetgum plantation after 11 years of CO_2–enrichment. Global Change Biol. 18, 1684–1697.

Jassal, R., Black, A., Novak, M., Morgenstern, K., Nesic, Z., Gaumont-Guay, D., 2005. Relationship between soil CO_2 concentrations and forest-floor CO_2 effluxes. Agric. For. Meteorol. 130, 176–192.

Jassal, R.S., Black, T.A., Drewitt, G.B., Novak, M.D., Gaumont-Guay, D., 2004. A model of the production and transport of CO_2 in soil: predicting soil CO_2 concentrations and CO_2 efflux from a forest floor. Agric. For. Meteorol. 124, 219–236.

Johnston, C.A., Groffman, P., Breshears, D.D., Cardon, Z.G., Currie, W., Emanuel, W., Gaudinski, J., Jackson, R.B., Lajtha, K., Nadelhoffer Jr., K., D.N, Post, W.M., Retallack, G., Wielopolski, L., 2004. Carbon cycling in soil. Front. Ecol. Environ. 10, 522–528.

Kane, E.S., Valentine, D.W., Michaelson, G.J., Fox, J.D., Ping, C., 2006. Controls over pathways of carbon efflux from soils along climate and black spruce productivity gradients in interior alaska. Soil Biol. Biochem. 38 (6), 1438–1450.

Kim, Y., Ueyama, M., Nakagawa, F., Tsunogai, U., Harazono, Y., 2007. Assessment of winter fluxes of CO_2 and CH_4 in boreal forest soils of central Alaska estimated by the profile method and the chamber method: a diagnosis of methane emission and implications for the regional carbon budget. Tellus B 59, 223–233.

Kirschbaum, M.U.F., 1995. The temperature dependence of soil organic matter decomposition and the effect of global warming on soil organic carbon storage. Soil Biol. Biochem. 27, 753–760.

Koehler, B., Corre, M.D., Steger, K., Well, R., Zehe, E., Sueta, J.P., Veldkamp, E., 2012. An in-depth look into a tropical lowland forest soil: nitrogen-addition effects on the contents of N_2O, CO_2 and CH_4 and N_2O isotopic signatures down to 2-m depth. Biogeochemistry 111, 695–713.

Kuchenbuch, R., Jung, J., 1988. Changes in root-shoot ratio and ion uptake of maize (Zea mays L.) from soil as influenced by a plant growth regulator. Plant soil 109, 151–157.

Kusa, K., Sawamoto, T., Hu, R., Hatano, R., 2010. Comparison of N_2O and CO_2 concentrations and fluxes in the soil profile between a Gray Lowland soil and an Andosol. Soil Sci. Plant Nutr. 56, 186–199.

Li, S.X., Xiao, L., 1992. Distribution and management of drylands in the People's Republic of China. Adv. Soil Sci. 18, 148–293.

Linn, D.M., Doran, J.W., 1984. Effect of water-filled pore space on carbon dioxide and nitrous oxide production in tilled and nontilled soils. Soil Sci. Soc. Am. J. 48, 1267–1272.

Liu, F., Liu, C.Q., Wang, S.L., Zhu, Z.J., 2012. Soil temperature and moisture controls on surface fluxes and profile concentrations of greenhouse gases in karst area in central part of Guizhou Province, southwest China. Environ. Earth Sci. 67, 1431–1439.

Liu, J.L., Zhan, A., Bu, L.D., Zhu, L., Luo, S.S., Chen, X.P., Cui, Z.L., Li, S.Q., Hill, R.L., Zhao, Y., 2014a. Understanding dry matter and Nitrogen accumulation for high-yielding film-mulched maize. Agron. J. 106, 390–396.

Liu, J.L., Zhu, L., Luo, S.S., Bu, L.D., Chen, X.P., Yue, S.C., Li, S.Q., 2014b. Response of nitrous oxide emission to soil mulching and nitrogen fertilization in semi-arid farmland. Agric. Ecosyst. Environ. 188, 20–28.

Liu, L., Greaver, T.L., 2009. A review of nitrogen enrichment effects on three biogenic GHGs: the CO_2 sink may be largely offset by stimulated N_2O and CH_4 emission. Ecol. Lett. 12 (10), 1103–1117.

Marshall, T.J., 1959. The diffusion of gas through porous media. J. Soil Sci. 10, 79–82.

Millington, R., Quirk, J.P., 1961. Permeability of porous solids. Trans. Faraday Soc. 57, 1200–1207.

Moldrup, P., Chamindu, D.T.K.K., Hamamoto, S., Komatsu, T., Kawamoto, K., Rolston, D.E., de Jonge, L.W., 2013. Structure-dependent water-induced linear reduction model for predicting gas diffusivity and tortuosity in repacked and intact soil. Vadose Zone J 12 (3), 155–175.

Moncrieff, J.B., Fang, C.F., 1999. A model for soil CO_2 production and transport 2: application to a florida pinus elliotte plantation. Agr. For. Meteorol. 95 (99), 237–256.

Mosier, A.R., Pendall, E., Morgan, J.A., 2003. Effect of water addition and nitrogen fertilization on the fluxes of CH_4 CO_2, NOx, and N_2O following five years of elevated CO_2 in the colorado shortgrass steppe. Atmos. Chem. Phys. 3 (suppl. 1), 1703–1708.

Nan, W.G., Yue, S.C., Huang, H.Z., Li, S.Q., Shen, Y.F., 2015. Effect of plastic film mulching on the distributions of greenhouse gases (CH_4, CO_2 and N_2O) within soil profiles in maize fields on the Loess plateau. China J. Integr. Agric. doi:http://dx.doi.org/10.1016/S2095-3119(15)61106-6.

Neff, J.C., Hooper, D.U., 2002. Vegetation and climate controls on potential CO_2, DOC and DON production in northern latitude soils. Global Change Biol. 8 (9), 872–884.

Novak, M.D., 2007. Determination of soil carbon dioxide source-density profiles by inversion from soil-profile gas concentrations and surface flux density for diffusion-dominated transport. Agric. For. Meteorol. 146, 189–204.

Ping, C.L., Michaelson, G.L., Dai, X.Y., Candler, R.J., 2001. Characterization of soil organic matter. In: Follett, R.F., Stewart, B.S. (Eds.), Assessment Methods for Soil Carbon. Lewis Publisher, London, pp. 273–283.

Pritchard, D.T., Currie, J.A., 1982. Diffusion coefficients of carbon dioxide, nitrous oxide, ethylene and ethane in air and their measurement. J. Soil Sci. 33, 175–184.

Ramirez, K.S., Lauber, C.L., Knight, R., Bradford, M.A., Fierer, N., 2010. Consistent effects of nitrogen fertilization on soil bacterial communities in contrasting systems. Ecology 91, 3463–3470.

Risk, D., Kellman, L., Beltrami, H., 2002a. Carbon dioxide in soil profiles: production and temperature dependence. Geophys. Res. Lett. 29, 11-1.

Risk, D., Kellman, L., Beltrami, H., 2002b. Soil CO_2 production and surface flux at four climate observatories in eastern Canada. Global Biogeochem. Cy. 16-1–69–12.

Rolston, D.E., 1986. Gas Flux, 47. American Society of Agronomy, Inc. Soil Science Society of America, Inc. Publisher, Madison, Wisconsin USA, pp. 1103–1109.

Rustad, L.E., Huntington, T.G., Boone, R.D., 2000. Controls on soil respiration: implications for climate change. Biogeochemistry 48, 1–6.

Schlesinger, W.H., Andrews, J.A., 2000. Soil respiration and the global carbon cycle. Biogeochemistry 48, 7–20.

Schulz, M., Stonestrom, D., Kiparski, G.V., Lawrence, C., Masiello, C., White, A., Fitzpatrick, J., 2011. Seasonal dynamics of CO_2 profiles across a soil chronosequence, santa cruz, california. Appl. Geochem. 26, S132–S134.

Shi, W.Y., Yan, M.J., Zhang, J.G., Guan, J.H., Du, S., 2014. Soil CO_2 emissions from five different types of land use on the semiarid Loess Plateau of China, with emphasis on the contribution of winter soil respiration. Atmos. Environ. 88, 74–82.

Shrestha, B.M., Sitaula, B.K., Singh, B.R., Bajracharya, R.M., 2004. Fluxes of CO_2 and CH_4 in soil profiles of a mountainous watershed of Nepal as influenced by land use temperature, moisture and substrate addition. Nutri. Cycl. Agroecosys. 68, 155–164.

Šimek, M., Hynšt, J., Šimek, P., 2014. Emissions of CH_4 CO_2, and N_2O from soil at a cattle overwintering area as affected by available C and N. Appl. Soil Ecol. 75, 52–62.

Tilman, D., Cassman, K.G., Matson, P.A., Naylor, R., Polasky, S., 2002. Agricultural sustainability and intensive production practices. Nature 418, 671–677.

Trumbore, S.E., 1993. Comparison of carbon dynamics in tropical and temperate soils using radiocarbon measurements. Global Biogeochem. Cycles 7, 275–290.

Vargas, V.P., Cantarella, H., Martins, A.A., Soares, J.R., Carmo, J.B., Andrade, C.A., 2014. Sugarcane crop residue increases N_2O and CO_2 emissions under high soil moisture conditions. Sugar Technol. 16, 174–179.

Wang, Y.Y., Hu, C., Ming, H., Oenema, O., Schaefer, D.A., Dong, W.X., Zhang, Y.M., Li, X. X., 2014. Methane, carbon dioxide and nitrous oxide fluxes in soil profile under a winter wheat-summer maize rotation in the North China Plain. PLoS One 9, e98445.

Wang, Y.Y., Hu, C.S., Ming, H., Zhang, Y.M., Li, X.X., Dong, W.X., Oenema, O., 2013. Concentration profiles of CH_4, CO_2 and N_2O in soils of a wheat–maize rotation ecosystem in North China Plain, measured weekly over a whole year. Agric. Ecosyst. Environ. 164, 260–272.

Williams, B.L., Edwards, A.C., 2006. Processes influencing dissolved organic nitrogen, phosphorus and sulphur in soils. Chem. Ecol. 8 (3), 203–215.

Wu, X., Yao, Z., Bruggemann, N., Shen, Z.Y., Wolf, B., Dannenmann, M., 2010. Effects of soil moisture and temperature on CO_2 and CH_4 soil-atmosphere exchange of various land use/cover types in a semi-arid grassland in Inner Mongolia. China Soil Biol. Biochem. 42, 773–787.

Xu, C.G., Chao, L., Wullschleger, S., Wilson, C., McDowell, N., 2011. Importance of feedback loops between soil inorganic nitrogen and microbial communities in the heterotrophic soil respiration response to global warming. Nat. Rev. Microbiol. 9 (3), 209–219.

Zhuang, J., Yu, G.R., Nakayama, K., 2001. Scaling of root length density of maize in the field profile. Plant Soil 235, 135–142.